Title
Psychosocial Stress Reactivity Is Associated With Decreased Whole-Brain Network Efficiency and Increased Amygdala Centrality

Journal
Behavioral Neuroscience, 132(6)

ISSN
0735-7044

Authors
Wheelock, Muriah D
Rangaprakash, Deshpande
Harnett, Nathaniel G
et al.

Publication Date
2018-12-01

DOI
10.1037/bne0000276

Peer reviewed

HHS Public Access

Author manuscript

Behav Neurosci. Author manuscript; available in PMC 2019 December 01.

Published in final edited form as:

Behav Neurosci. 2018 December ; 132(6): 561–572. doi:10.1037/bne0000276.

Psychosocial stress reactivity is associated with decreased whole brain network efficiency and increased amygdala centrality

Muriah D. Wheelock[1], **Desphande Rangaprakash**[2,3], **Nathaniel G. Harnett**[1], **Kimberly H. Wood**[1], **Tyler R. Orem**[1], **Sylvie Mrug**[1], **Douglas A. Granger**[4,5], **Gopikrishna Deshpande**[2,3,6,7], and **David C. Knight**[1,7]

[1]Department of Psychology, University of Alabama at Birmingham, AL, USA

[2]Auburn University MRI Research Center, Department of Electrical and Computer Engineering, Auburn University, AL, USA

[3]Semel Institute for Neuroscience and Human Behavior, University of California, Los Angeles, Ca, USA

[4]Institute for Interdisciplinary Salivary Bioscience Research & Center for the Neurobiology of Learning and Memory University of California, Irvine

[5]Johns Hopkins University School of Nursing, Johns Hopkins University Bloomberg School of Public Health, and Johns Hopkins University School of Medicine, Baltimore, MD, USA

[6]Department of Psychology, Auburn University, AL, USA

[7]Alabama Advanced Imaging Consortium, Auburn University and University of Alabama at Birmingham, Birmingham, AL, USA

Abstract

Cognitive and emotional functions are supported by the coordinated activity of a distributed network of brain regions. This coordinated activity may be disrupted by psychosocial stress, resulting in the dysfunction of cognitive and emotional processes. Graph theory is a mathematical approach to assess coordinated brain activity that can estimate the efficiency of information flow and determine the centrality of brain regions within a larger distributed neural network. However, limited research has applied graph theory techniques to the study of stress. Advancing our understanding of the impact stress has on global brain networks may provide new insight into factors that influence individual differences in stress susceptibility. Therefore, the present study examined the brain connectivity of participants that completed the Montreal Imaging Stress Task. Salivary cortisol, heart rate, skin conductance response, and self-reported stress served as indices of stress, and trait anxiety served as an index of participant's disposition towards negative

To whom correspondence should be addressed: David C. Knight, Ph.D, Department of Psychology, University of Alabama at Birmingham, CIRC 235H, 1720 2nd Ave S, Birmingham, AL 35294, 205-996-6344, knightdc@uab.edu.

Note: Current Affiliation for Dr. Kimberly H. Wood is the Dept. of Psychology at Samford University, Birmingham, AL

Disclosure Statement: In the interest of full disclosure, DAG is founder and Chief Scientific and Strategy Advisor at Salimetrics LLC and Salivabio LLC. These relationships are Managed by the policies on conflict of interest at the Johns Hopkins University School of Medicine and the University of California at Irvine.

affectivity. Psychosocial stress was associated with a decrease in the efficiency of the flow of information within the brain. Further, the centrality of brain regions that mediate emotion regulation processes (hippocampus, ventral prefrontal cortex, and cingulate cortex) decreased during stress exposure. Interestingly, individual differences in cortisol reactivity were negatively correlated with the efficiency of information flow within this network, whereas cortisol reactivity was positively correlated with the centrality of the amygdala within the network. These findings suggest that stress reduces the efficiency of information transfer and leaves the function of brain regions that regulate the stress response vulnerable to disruption.

Keywords

graph theory; stress; amygdala; cortisol; network efficiency; brain connectivity

1.0 Introduction

Stress is typically considered an adaptive response to adverse life events (Chrousos, 2009). However, high levels of prolonged stress can have deleterious effects on mental health. Stress also produces a range of psychophysiological responses (e.g., cortisol, cardiac, skin conductance, and respiratory responses) that show large inter-individual variability. For example, while some individuals show a large emotional response to stress, others are relatively nonreactive (Negrao, Deuster, Gold, Singh, & Chrousos, 2000). Differences in the brain function that underlies stress reactivity may account for the individual variability observed in the emotional response to stress. For example, dysfunction of the network of brain regions that regulate hypothalamic-pituitary-adrenal (HPA) axis activity appears to predispose certain individuals to immune, cardiovascular, metabolic, and psychiatric disorders (Chrousos, 2009; Franklin, Saab, & Mansuy, 2012). Therefore, understanding the brain function that underlies individual differences in stress reactivity and susceptibility may ultimately have important implications for the social and economic burden of stress-related disorders.

Psychosocial stress research has largely focused on understanding hypothalamic-pituitary-adrenal (HPA) axis activity (Chrousos & Gold, 1992) as this pathway controls the production of cortisol (Chrousos, 1998; Nicolaides, Kyratzi, Lamprokostopoulou, Chrousos, & Charmandari, 2015). However, contemporary theory suggests that cognitive and emotional deficits result from disruptions in brain connectivity across large networks of distributed brain regions. Brain regions that include the dorsal prefrontal cortex (PFC), ventral PFC, hippocampus, and amygdala contain cortisol receptors and mediate important processes that support the perception, interpretation, and emotional response to stress (Oken, Chamine, & Wakeland, 2015). Specifically, prior work suggests the PFC and hippocampus exert inhibitory control over the HPA axis, while the amygdala exerts an excitatory influence over HPA axis function. Thus, a complex brain network appears to influence an individual's biological sensitivity to stress, and may ultimately mediate intra-individual differences in susceptibility to stress-related psychiatric disorders (Cisler et al., 2013; Holsen et al., 2013; Schatzberg et al., 2014; van der Werff, Pannekoek, Stein, & van der Wee, 2013; Veer et al.,

2011). However, few studies to date have assessed the relationship between stress and the connectivity of large-scale complex brain networks.

While traditional connectivity approaches quantify the relationship between pairs of brain regions, they fail to elucidate the organizational structure and degree of communication among an ensemble of connections (Rubinov & Sporns, 2010). Graph theoretical methods can be used to characterize the flow of information within complex brain networks and provide additional unique information not obtainable through traditional connectivity analyses. Of the many metrics to quantify network topology (i.e. information flow), global efficiency provides compelling information about the functional integration and parallel information transfer within the brain during stress (Rubinov & Sporns, 2010). Further, measures of regional centrality (e.g. node betweenness) provide insight into which brain regions are most integral to information transfer within a network (Rubinov & Sporns, 2010).

The present study investigated the relationship between stress-related psychobiological processes and brain network topology using an adaptation of the Montreal Imaging Stress Task (MIST) (Goodman et al., 2016; Wheelock et al., 2016). Functional magnetic resonance imaging (fMRI) data were collected during the MIST to examine network connectivity, and psychophysiological data (i.e. cortisol, heart rate, and skin conductance response) to determine the relationship between network connectivity and the peripheral emotional response. We hypothesized that (i) psychosocial stress would decrease whole-brain global network efficiency, (ii) psychosocial stress would reduce the centrality of brain regions (e.g. PFC and hippocampus) that regulate the emotional response (e.g. cortisol) to stress, (iii) stress would increase the centrality of brain regions (e.g. amygdala) that support the peripheral expression of the emotional response to stress, and (iv) individual variability in the emotional response to stress would vary with brain network efficiency and the centrality of the amygdala within the network during psychosocial stress.

2.0 Materials and Methods

2.1 Participants

One hundred and twenty right-handed volunteers participated in this study as part of a larger project that involved a community sample. 52 of these participants were included in a previously published neuroimaging study of stress (Wheelock et al., 2016). In the present analysis, four subjects were excluded due to an affective disorder diagnosis, six subjects were excluded due to incomplete imaging data, one subject was excluded for incidental findings (i.e. brain abnormality), and one subject was excluded for failure to follow instructions. Thus, 108 subjects (57 males: M age=18.88 years, range 17–22 years) were included in the present analyses. All subjects provided written informed consent as approved by the University of Alabama at Birmingham Institutional Review Board.

2.2 Task design

Participants completed a modified version of the MIST, a challenging mental arithmetic task optimized for administration during fMRI (Dedovic et al., 2005). Detailed methods for the

MIST are reported elsewhere (Goodman et al., 2016; Wheelock et al., 2016). Briefly, the MIST used in the present study was a fast event-related design consisting of two scans (a 'Control' and a 'Stress' scan). Each scan was 7 minutes 54 seconds in duration and contained 54 trials. Each trial lasted six seconds. At the start of the trial a unique math problem was presented along with response options (0–9) that the participant could select. After response selection (button press) a fixation cross appeared (0.5–5 seconds duration) followed by 0.5 seconds of visual feedback ("Right", "Wrong", or "Time out"). Each trial was separated by a fixation cross during a variable inter-trial-interval (1–3 seconds). Math in the MIST consisted of either easy (two integers) or medium-easy (three integer) addition and subtraction problems. Prior to the scanning session, participants completed practice math problems and, based on individual performance, the difficulty level (either receiving two or three integer math problems) for the MRI task was determined for each subject. For each participant, the difficulty level (easy or medium-easy math problems) remained constant across Control and Stress scans.

Prior to the Control scan, investigators attempted to lower participant stress levels by telling them "It is OK if you do not answer all of the math problems correctly." During the Control scan the participants were given five seconds in which to respond to each math problem. Further, during the Control scan, participants were given previously recorded positive auditory feedback. In contrast, the investigators attempted to elevate stress levels prior to the Stress scan by telling participants they must answer the questions correctly, and warning that if they did not perform as well as others in the study their data would not be used. In addition, participants were told that prior subjects answered more than 80% of the answers correctly, and if he/she did not answer at least 80% correct his/her data would not be used. Further, during the Stress scan, the participants were given recorded negative auditory feedback. Failure during the Stress scan was ensured by modulating the time in which the participant could respond in a stair-step manner such that on average participants answered approximately 50% of the problems correctly.

2.3 Task presentation

Presentation software (Neurobehavioral Systems, Inc.; Albany, CA) was used to present the visual stimuli through an IFIS-SA LCD (Invivo Corp.; Gainesville, FL) video screen located above the participant's head. The participants were able to view the video screen through a mirror attached to the RF coil. Participants used an MRI compatible joystick (Current Designs; Philadelphia, PA) to highlight their math answer and a button on the joystick to make their selection. Participants' responses to the math problems were used to provide corresponding real time visual feedback on task performance (e.g. 'Right', 'Wrong', or 'Time out'). Prerecorded auditory feedback was presented at four fixed points (i.e. after the first 4 sets of 9 trials) during each scan through MR-compatible pneumatic headphones.

2.4 Trait Anxiety

Prior work indicates network connectivity is altered in individuals with high negative affect and anxiety (Hermans et al., 2011; McMenamin, Langeslag, Sirbu, Padmala, & Pessoa, 2014). Therefore, participants completed the State-Trait Anxiety Inventory (STAI form Y, Spielberger, 1983) prior to the imaging session. Scores on the trait anxiety scale were

assessed as an index of participants' general tendency to engage in negative affect, and used for comparison to the neural response to stress.

2.5 Self-Reported Stress

A measure of self-reported stress level was developed as a manipulation check of participant's emotional response to Control and Stress MIST scans. Following the completion of the MIST, participants completed a self-report questionnaire consisting of eight statements. Participants rated each statement's applicability on a five-point scale where 1 corresponded to "not at all" and 5 corresponded to "Extremely". Four of the statements were worded positively (e.g. I felt calm) and four were worded negatively (e.g. I felt stressed) for a total possible self-reported stress score of 40 (Wheelock et al., 2016).

2.6 Math performance

Math task performance was assessed as a manipulation check to confirm that task performance varied between Control and Stress MIST scans as designed. While the difficulty of math problems remained constant for each participant, the response time window was titrated during Stress MIST to obtain an approximately 50% performance level. Therefore, math task performance was calculated as the percentage of correct answers during Control and Stress MIST.

2.7 Skin Conductance Response

Skin conductance response (SCR) data were collected using an MRI compatible physiological monitoring system (Biopac Systems; Goleta, CA) using the basic methodology described in prior work (Knight & Wood, 2011). SCR was sampled at 10 kHz with a pair of disposable radio-translucent electrodes (1 mm diameter, Biopac Systems; Goleta, CA) located on the thenar and hypothenar eminence of the non-dominant hand. SCR data were low pass filtered at 1Hz and downsampled to 250 Hz using Acqknowledge 4.1.0 software. The downsampled SCR were analyzed with SCRalyze toolbox (version b2.1.8) (Bach, Flandin, Friston, & Dolan, 2009). The data were then bandpass filtered with a first order Butterworth filter (highpass cutoff of 0.0159 Hz, lowpass filter of 1.0 Hz), downsampled to a 10 Hz sampling rate, and the time-series was normalized (z-transformed and mean centered). SCRs to math events were estimated using the general linear model with an assumed SCR function without a time or dispersion derivative.

2.8 Heart Rate

Heart rate (HR) was collected using an MR compatible photoplethysmograph placed on the index finger of the non-dominant hand. Heart rate was recorded at 50Hz using a Siemens Physiological Monitoring Unit. QRSTool was used to identify peaks in the pulse waveform (Allen, Chambers, & Towers, 2007). CMetX was used to calculate the average HR for Stress and Control scans (Allen et al., 2007).

2.9 Cortisol Analysis

Two saliva samples were collected to assess the cortisol response to the MIST. Whole saliva samples (1.0 ml) were collected using passive drool through a short straw into 2.0 ml

cryovials, then stored at −80C until the day of assay. The first sample (Time1) was collected prior to the scanning session and the second sample (Time 2) was collected 20 minutes following the MIST. Samples were assayed at the Institute for Interdisciplinary Salivary Bioscience Research using a commercially available cortisol immunoassay kit without modification to the manufacturer's recommended protocol (Salimetrics, LLC in State College, PA). The cortisol assay used 25 ul of saliva for singlet determinations. The assay had a lower limit of sensitivity of .007 ug/dL (range to 3.0 ug/dL), and intra- and inter-assay coefficients of variation were, on average, less than 5 and 15 % respectively. Samples were assayed in duplicate and the average of the duplicate assays was used in the statistical analyses. Cortisol data were transformed to nmol/L and cortisol outliers were assessed. Subjects with raw cortisol data greater than 3SD from the mean on both pre- and post-MIST samples were excluded. Cortisol reactivity was calculated as the difference between post- and pre-MIST cortisol. Cortisol reactivity outliers (greater than 3SD from the mean) were assessed and winsorized at the 97th percentile prior to further statistical analyses. The effect of the MIST on baseline (Time 1) to post-stress (Time 2) cortisol levels was assessed for the whole group using a 1-way repeated measures ANCOVA (including time of day as a covariate). Furthermore, intersubject variability in cortisol reactivity attributable to behavioral measures including trait anxiety, self-reported stress ratings, HR, and SCR was assessed using Pearson correlations.

2.10 Functional MRI acquisition

Functional MRI data were acquired on a 3T Siemens Allegra scanner using a gradient recalled echo-planar imaging (EPI) sequence (TR = 2000ms, TE = 30ms, flip angle = 70°, FOV = 24cm, matrix = 64X64, slice thickness = 4mm). A T1-weighted magnetization prepared rapid acquisition gradient-echo sequence (MPRAGE) reference image was acquired in the sagittal plane (TR = 2300 ms, TE = 3.9 ms, flip angle = 12°, FOV = 25.6 cm, matrix = 256×256, slice thickness = 1 mm, 0.5 mm gap).

2.11 Identification of regions of interest

Regions of interest (ROI) for effective connectivity analyses were selected based on previously published neuroimaging findings from our lab using the MIST (Wheelock et al., 2016). In this prior work, MRI data were preprocessed in AFNI (Cox, 1996). The fMRI data were corrected for motion by censoring high motion TRs and including nuisance regressors for the six head motion parameters. Functional MRI data were deconvolved with a duration modulated (based on response time to math problems) gamma variate hemodynamic response function and normalized to MNI space. A multiple linear regression analysis (3dttest++) was used to determine the relationship stress (i.e. contrast of fMRI signal elicited by Math problems during Stress vs Control conditions) has to trait anxiety, self-reported stress, and cortisol reactivity. **However, similar analyses were not completed with HR and SCR in this prior project.** Analyses were restricted to grey matter and were cluster corrected using FWE $p<0.05$. Peak activation coordinates from each atlas region were identified using WFU PickAtlas (Maldjian, Laurienti, Burdette, & Kraft, 2003), resulting in 105 coordinates of interest (Wheelock et al., 2016). 4 mm radius spheres were placed at the 105 coordinate locations. **These 105 ROI were selected based on areas of activation in prior published work (Wheelock et al., 2016). Thus, regions of unilateral activation do**

not have a corresponding ROI in the contralateral hemisphere. Further, the right amygdala coordinate was shifted so that the coordinate center and the extent of the 4mm radius sphere fell entirely within the anatomical boundaries of the amygdala. An a priori left amygdala coordinate was added at the same location in the left hemisphere. This resulted in a final ROI count of 106 coordinates (54 left hemisphere, 52 right hemisphere) (Supplemental Table S1, Supplemental Figure S1).

2.12 Effective Connectivity Analysis

The **entire, raw** mean time series from the 4mm radius spheres centered on the 106 coordinates were extracted **from Stress and Control scans** for all participants. Because research suggests vascular differences across regions of the brain can spuriously influence effective connectivity estimates (Webb, Ferguson, Nielsen, & Anderson, 2013), deconvolution was used to remove hemodynamic differences between time series from each ROI (David et al., 2008; Deshpande & Hu, 2012; Deshpande, Sathian, & Hu, 2010; Grant et al., 2015; Sreenivasan, Havlicek, & Deshpande, 2015). Therefore, the average time series from each ROI were temporally normalized and the corresponding latent neuronal signals were obtained via blind hemodynamic deconvolution of the fMRI time series using a cubature Kalman filter (Havlicek, Friston, Jan, Brazdil, & Calhoun, 2011). **Deconvolution was performed by modeling each of the task events (i.e. math presentation, visual feedback, fixation, and auditory feedback events).** Because deconvolution removes the hemodynamic response from the time series, no vascular or non-neuronal effects remain in the time series. Granger causality (Granger, 1969) was implemented using a dynamic multivariate autoregressive model to assess the causal influence of one brain region on another. This model dynamically estimates causal relationships between the deconvolved time series of pairs of regions across the entire duration of the task (for both Control and Stress conditions) (Grant et al., 2015; Havlicek, Jan, Brazdil, & Calhoun, 2010; Wang, Katwal, Rogers, Gore, & Deshpande, 2016). All possible pairwise effective connections were obtained between all 106 regions **during math trials for Control and Stress scans** for each subject, which produced the weighted directed networks used in further graph theoretic analyses. Details of the effective connectivity model and deconvolution have been reported previously (Wheelock et al., 2014). The effective connectivity methods in the present paper produced weighted directed networks.

2.13 Graph Metrics

Many graph metrics are best estimated when the connections between nodes are sparsely connected. Sparse graphs can be generated by thresholding the graph such that only the strongest network connections remain. The effective connectivity networks in the present analysis were systematically thresholded across a range of network edge densities to produce the graph metrics of interest (i.e. global efficiency and nodal betweeness centrality) (Hosseini, Hoeft, & Kesler, 2012; Wang et al., 2015; Zhang et al., 2011). For each subject, the area under the curve (AUC) from the range of network edge densities was used as a single summary graph metric to reduce the number of comparisons assessed. A range of network edge densities (1% to 40% in 1% increments) were used to generate these curves. Graph Theoretical Network Analysis toolbox (GRETNA version 1.2.1) (Wang et al., 2015) was used to analyze the subject matrices and produce the AUC and graph metrics of interest.

Outliers in graph metrics were assessed at 3 standard deviations above or below the mean, and were winsorized at the 97th percentile prior to further statistical analyses. BrainNetViewer (version 1.42) was used to display nodes for illustration purposes (Xia, Wang, & He, 2013).

2.13.1 Network Efficiency.—Efficiency is a measure of functional integration and parallel information transfer within a network. Functional integration within the brain allows rapid communication and transfer of information across distributed brain regions. On a global scale, efficiency can be defined mathematically as the average inverse shortest path length in the network, where path length is defined as the fewest number of edges between nodes. Low global efficiency reflects the use of long indirect neural pathways to transfer information across distributed brain regions. In the present study, global efficiency was calculated for each subject using the AUC estimate of network efficiency at a range of network densities (1%−40%). Paired samples t-tests were used to compare AUC global efficiency between Stress and Control conditions. **Further, psychobiological measures (i.e. trait anxiety, self-reported stress, cortisol reactivity, HR, and SCR) were compared (i.e., using Pearson's correlations) to global efficiency during the Stress as well as the contrast between Stress and Control conditions. Graph metrics were assessed during Stress as an index of brain communication under stress, as well as during the comparison of Stress-Control conditions. The comparison of Stress-Control conditions assessed whether graph metrics differed between these conditions, while the analysis of the Stress condition alone provides an additional confirmatory analysis that differential effects observed in the Stress-Control contrast are truly due to stress-induced, rather than control condition effects.** Correlations were Bonferroni corrected to control familywise error rates.

2.13.2 Node Centrality.—The relative importance of a given node to information transfer within the network was assessed using node betweenness centrality. Betweenness centrality was calculated as the degree to which a given node mediates the number of shortest paths from all other regions. A region with low betweenness centrality contributes relatively little to information transfer within the network, while a high betweeness centrality score indicates a region is relatively important for information flow. **AUC was used to assess node betweenness during the Stress condition as well as the contrast between Stress and Control conditions.** Differences in node betweenness were assessed for a set of 12 *a priori* brain regions (a subset of the entire graph) using paired samples t-tests to compare Control and Stress conditions. *A priori* regions of interest were selected **from the 106 regions identified above** (Supplemental Table S1, Supplemental Figure S1), **and restricted to areas identified** in prior stress and emotion regulation research (Dedovic, Duchesne, Andrews, Engert, & Pruessner, 2009; Hartley & Phelps, 2010). **These 12 ROI** included 2 amygdala, 2 hippocampal, 5 vmPFC, and 3 dmPFC regions. FDR correction was used to control familywise error rates in comparisons of these *a priori* regions of interest (Benjamini & Hochberg, 1995). Further, given that node betweenness of the amygdala was of particular interest, amygdala node betweenness was correlated with psychobiological data (i.e. trait anxiety, self-reported stress, cortisol reactivity, HR, and SCR) to assess the

influence of amygdala node centrality on the stress response. Correlations were Bonferroni corrected to control familywise error rates.

3.0 Results

3.1 State and Trait Anxiety

The State (Mean=32.10, SEM=0.84, Range=20–56) and Trait (Mean=34.22, SEM=0.83, Range=20–57) Anxiety Inventory (Spielberger, 1983) was completed as an index of negative affect prior to the scanning session. State and Trait anxiety inventory scores were correlated ($r=0.488$, $p<0.001$, $R^2=0.238$). Trait anxiety was used as an index of general negative affect in comparisons with behavioral and brain network topological data.

3.2 Skin Conductance Response

SCR was monitored during the scanning session as an index of the peripheral emotional response to Stress and Control MIST. Nineteen individuals had no measurable SCRs (i.e. zero SCRs above 0.05 μSiemens). Thus, data from these participants were excluded from SCR analyses. Paired t-test comparisons revealed that SCRs to math events were significantly greater during Stress than Control conditions (Table 1). These data demonstrate differential SCR to Stress vs. Control scans, and provide behavioral evidence the Stress condition was more stressful than the Control condition.

3.3 Heart Rate

HR was also monitored during the scanning session to assess the differential emotional response to Stress and Control MIST. HR data were not collected from 13 subjects due to equipment malfunction. In addition, HR could not be calculated for 26 participants due to excessive noise in the signal. Paired t-test comparisons indicate HR was significantly higher during Stress than Control MIST (Table 1). These data demonstrate differential cardiac response to Stress vs. Control scans, and provided additional behavioral evidence the Stress condition was more stressful than the Control condition.

3.4 Self-Reported Stress

Ratings of self-reported stress were obtained for Control and Stress conditions of the MIST. Self-reported stress was not collected for 12 participants. Thus, self-reported stress data for these participants were not included in these analyses. Paired t-test comparisons of self-reported stress indicate that participants found the Stress condition more stressful than the Control condition (Table 1). **Due to missing data across measures, paired samples t-tests were also run excluding cases listwise, which demonstrated the same pattern of results** (Supplemental Table S2).

3.5 Cortisol

One subject did not have cortisol data (saliva was too viscous for assay), and could not be included in analyses. One subject was an extreme outlier on both pre- and post-MIST cortisol samples (greater than 3SD) and was excluded from further analyses. Thus cortisol data from 106 subjects were analyzed. **Repeated measures ANCOVA revealed no-**

significant change in cortisol from baseline to post-MIST when covarying for time of day ($F(1)=0.350$, $p>0.05$) nor a significant interaction of time of day and cortisol ($F(1) = 0.0$,$p>0.05$). However, as with prior stress research, considerable heterogeneity was observed in inter-individual cortisol levels. Following previously published guidelines we defined a difference between pre and post-scan cortisol values greater than 10% *and* at least an absolute difference of 0.55 nmol/L as cortisol reactivity (i.e., a difference this large is 2× the average intra-assay coefficient of variation and 2× the lower limit of detection) (Granger et al., 2012). Using this criterion, 23 of 106 participants showed increases in cortisol in response to the MIST. Within this group the mean increase in cortisol T1 to T2 was 3.27 (SEM=0.68) nmol/L or 66.73%. Cortisol reactivity, self-reported stress, trait anxiety scale scores, HR reactivity, and SCR reactivity were not correlated ($p > 0.05$), **nor were they significantly correlated when controlling for time of day of cortisol collection (> 0.05)**. The effect of gender and race on cortisol reactivity, self-reported stress, trait anxiety, HR reactivity, and SCR reactivity was assessed and found to be non-significant $p>0.05$.

3.6 Math Performance

The percentage of correctly answered items during Control and Stress scans was calculated as a manipulation check. During the Control scan, participants answered 86% correct (range 57–100%, SEM=0.01), whereas participants only answered 54% correct (range 44–57%, SEM=0.01) on the Stress scan (Table 1). These findings confirm that performance varied across scans as designed.

3.7 Network Connectivity

Seventeen subjects were excluded from the network connectivity analyses (two subjects were missing data from more than one node and fifteen subjects had poor fitting deconvolution models). Thus, 91 subjects were included in network connectivity group level analyses.

3.7.1 Efficiency.—

Whole brain global efficiency was assessed to examine the impact of stress on efficient network processing. Global network efficiency was significantly lower during Stress than Control conditions at a range of network densities (3%−31%) (Figure 1A). Paired samples t-test of the AUC of global efficiency across network densities revealed that network efficiency was significantly lower during the Stress than Control condition ($t(90)=-8.16$, $p<0.001$) (Figure 1B). In addition, a correlation analysis was completed to compare network efficiency with individual variability in psychobiological characteristics. Network global efficiency during the Stress condition was negatively correlated with individual variability in cortisol reactivity **($r=-.282$, $p<0.005$)** (calculated as the difference from pre- to post-MIST cortisol) (Table 2, Figure 1C). Whole brain global efficiency did not correlate with any other psychobiological data. **Due to the variability in the number of subjects with usable data from each psychological and biological measure, the association between global efficiency and each psychobiological variable was also assessed limiting cases listwise. When limiting cases listwise (n=44), over half the sample was excluded, and cortisol reactivity was no longer significantly associated with global efficiency** (Table S3).

3.7.2 Node Betweenness Centrality.—Node betweenness centrality was assessed using AUC for each individual during Control and Stress conditions. Node betweenness centrality was decreased for the left ventromedial prefrontal cortex (vmPFC) and left hippocampus in the Stress compared to Control condition ($p<0.05$ FDR corrected) (Table 3, Figure 2). A trend toward a decrease in node betweenness centrality was also observed within the right rostral and dorsal anterior cingulate cortex (Table 3). Although amygdala betweenness did not differ between the Control and Stress MIST conditions ($p>0.05$), intersubject variability in amygdala betweenness (Stress-Control conditions) was positively correlated with cortisol reactivity (Table 4, Figure 3). Amygdala betweeness centrality did not correlate with any other psychobiological data. **The association between amygdala betweenness centrality and each psychobiological variable was also assessed limiting cases listwise. Cortisol reactivity remained significantly associated with amygdala betweenness after removing cases listwise (n=44;** Table S4).

4.0 Discussion

Stress exposure influences the structure and function of brain connectivity (McEwen & Gianaros, 2011). However, limited prior research has investigated the impact of acute stress on network topology. In this study we investigated the topology of a large network of brain regions identified in prior psychosocial stress research (Wheelock et al., 2016). We found that global network efficiency decreased during psychosocial stress compared to the control condition. Further, global network efficiency during stress varied with cortisol reactivity. Specifically, as global network efficiency decreased, stress reactivity (indexed via cortisol) increased. We also evaluated an *a priori* subset of 12 brain regions within the emotion regulation network and demonstrated decreased network centrality (measured using betweenness) during Stress compared to Control MIST within the hippocampus and vmPFC. Finally, amygdala betweenness centrality during Stress compared to Control conditions was positively correlated with individual variability in cortisol reactivity.

4.1 Stress reactivity

Stress reactivity was assessed using a variety of psychological and psychophysiological measures in the present study. In addition to salivary cortisol, we measured HR, SCR, and self-reported stress, as well as trait anxiety as a measure of the general disposition towards negative affectivity. These psychobiological measures did not correlate with one another, suggesting each of these measures indexes a distinct facet of the stress response. Further, while cortisol reactivity explained variance in global network efficiency and amygdala betweeness centrality, HR, SCR, and self-reported stress did not explain variance in these network connectivity metrics. Taken together, these findings suggest that whole brain global efficiency and amygdala betweeness centrality play a distinct psychobiological role in mediating individual variability in cortisol reactivity to psychosocial stress.

4.2 Network Efficiency

In the present paper, network efficiency was assessed as a metric of functional integration and parallel information transfer within the brain. Functional integration within the brain allows rapid communication and information transfer across distributed brain regions. We

observed decreased global network efficiency during psychosocial stress as compared to our control condition. **While math difficulty was the same during both the Stress and Control conditions, one might speculate that reducing the time available for participants to respond could increase cognitive demands during the Stress condition. However, prior research suggests that cognitively demanding tasks (e.g. N-Back task) increase global efficiency relative to simpler tasks (e.g. finger tapping) or resting state** (Cohen & D'Esposito, 2016). **Further, prior research suggests that modulating the level of cognitive demand during an n-back task does not alter global efficiency** (Ginestet & Simmons, 2011). **Thus, increased cognitive demand during the Stress condition of the present study, should either increase or produce no difference in global efficiency. These expectations are inconsistent with the global efficiency results obtained in the present study. Instead, the current findings demonstrate reduced global efficiency during the Stress condition. These findings suggest that stress reduces the efficiency of neural communication, as opposed to the view that greater cognitive demand increases the efficiency of communication within the brain**.

In addition to observing reduced global efficiency during the stress scan, we also observed that individual variability in network efficiency during the stress condition was negatively correlated with individual variability in stress reactivity. Specifically, individuals with the lowest network efficiency during stress were the most stress reactive (as indexed by salivary cortisol). Taken together, these findings suggest that psychosocial stress disrupts network efficiency, and in turn, disrupted network efficiency leads to increased cortisol release. Prior work indicates that acute stress is associated with deficits in concentration, problem-solving, decision making, reasoning, maintaining selective and divided attention, spatial working memory, and memory recall (Joels, Pu, Wiegert, Oitzl, & Krugers, 2006; Kirschbaum, Wolf, May, Wippich, & Hellhammer, 1996; Leach, 2004; Lupien, Maheu, Tu, Fiocco, & Schramek, 2007; Schwabe & Wolf, 2010; Vedhara, Hyde, Gilchrist, Tytherleigh, & Plummer, 2000). These stress-related cognitive deficits may be linked to decreased communication among brain regions (i.e. decreased functional integration) during stress as observed in the present study. Furthermore, individuals with the poorest functional integration across brain regions have the greatest release of endogenous cortisol. This finding suggests that greater endocrine reactivity to stress is a product of the degree to which brain communication is efficient (or inefficient) during an acute stressor. Prior research suggests that the stress-related neural disconnectivity observed in the present study is mediated by altered receptor trafficking and dendritic spine morphology (Sousa & Almeida, 2012). However, prior neuroimaging research has not previously assessed stress-induced neural disconnectivity at the cognitive/systems level using an experimental stress manipulation in humans. The present findings support the view that stress disrupts efficient functional network connectivity.

4.3 Node Centrality

Node centrality was assessed for a subset of 12 *a priori* ROI including the dmPFC, vmPFC, cingulate, hippocampus, and amygdala using an estimate of node betweenness. The left hippocampus and vmPFC demonstrated decreased betweenness centrality during Stress compared to Control MIST. This finding is consistent with research suggesting the vmPFC

and hippocampus play an important role in the regulation of the emotional response to stress (Jankord & Herman, 2008). The decreased betweenness centrality of these nodes during stress may reflect the impact of stress on emotion regulation circuitry. Specifically, decreased betweenness centrality of the vmPFC and hippocampus during stress suggests these brain regions have a decreased role in regulating the function of other brain regions during stress, resulting in decreased inhibition of the HPA axis. We did not observe an increase in amygdala betweeness centrality during stress as hypothesized. However, differential amygdala betweenness (Stress-Control betweenness) was positively correlated with individual variability in stress reactivity. Specifically, individuals with greater amygdala betweenness centrality during Stress compared to Control conditions demonstrated greater stress reactivity. These findings suggest the degree to which the amygdala mediates information flow within the brain impacts individual variability of the stress response. Taken together, these data are consistent with animal model research that has demonstrated stress enhances amygdala function while decreasing PFC function (Arnsten, 2015; Arnsten, Raskind, Taylor, & Connor, 2015). While prior research has observed a relationship between amygdala centrality and negative affectivity (Zhang, Li, & Pan, 2015), we did not observe any association between trait anxiety scores and amygdala centrality in the present study. However, this study does suggest the amygdala is a central component of the neural network that mediates cortisol reactivity in response to acute stress.

5.0 Limitations

In the present study, we did not observe an increase in cortisol from pre to post-stress. This finding is inconsistent with prior stress research, which has typically shown a robust cortisol response to psychosocial stress tasks (Kirschbaum, Pirke, & Hellhammer, 1993). However, prior neuroimaging research suggests that stress tasks performed in the MRI environment do not reliably produce a strong cortisol response (Allendorfer et al., 2014; Dedovic et al., 2014; Dedovic, Rexroth, et al., 2009; Goodman et al., 2016; van Marle, Hermans, Qin, & Fernandez, 2010; Wheelock et al., 2016). Instead, there appears to be increased heterogeneity of the cortisol response during fMRI, which may be due to many factors including the novel environment, medical procedure, social evaluative threat associated with the scan procedure itself, loss of control, loud and startling noises, isolation, and confinement (Gossett et al., 2018). Thus, participants may perceive the MRI environment and testing procedures in the present study as a threatening experience, which would in turn, elevate baseline measurements of cortisol prior to the start of stress task. However, research suggests that inter-individual variability in endogenous cortisol levels, whether increasing or decreasing over the task, explain meaningful variance in brain connectivity between brain regions that regulate the stress response (Veer et al., 2012). Therefore, despite the non-significant increase in cortisol across participants in the present study, the authors suggest that meaningful information about brain communication associated with the stress response can still be inferred. In the present study, approximately 22% of participants demonstrated elevated cortisol levels post-stress. Ideally, we would have been able to demonstrate increases in cortisol in a majority of participants following stress exposure to provide psychophysiological evidence that the task was indeed stressful. However, our other self-report and psychophysiological measures (i.e. stress ratings, HR, SCR) do provide strong

evidence that participants found the task stressful (Wheelock et al., 2016). Future research should consider study designs that overcome the inherent stress of the scanning environment by combining approaches from psychosocial stress paradigms, physical stressors, and unpredictable stress (Quaedflieg, Meyer, & Smeets, 2013).

6.0 Conclusions

This study assessed the impact of stress on brain connectivity using graph theory techniques. While psychobiological reactivity increased (HR, SCR, and self-reported stress), network efficiency decreased during Stress compared to Control conditions of the MIST. These findings suggests that stress disrupts efficient information transfer within the brain. In addition, acute psychosocial stress decreased the centrality of nodes that regulate the stress response (e.g. vmPFC and hippocampus). In contrast, stress increased the centrality of the amygdala within the information processing network of high stress individuals. Taken together these findings suggest neurobiological mechanisms by which stress alters network topology. These stress induced vulnerabilities in network connectivity may precipitate the development of psychiatric illness. Future research should consider examining the utility of graph theory metrics of brain network topology as biomarkers to predict individual risk for the development of stress-related psychiatric illnesses.

Supplementary Material

Refer to Web version on PubMed Central for supplementary material.

Acknowledgments

Funding

This study was supported by National Institutes of Health (grant number MH098348 to SM & DCK).

References

Allen JJ, Chambers AS, & Towers DN (2007). The many metrics of cardiac chronotropy: a pragmatic primer and a brief comparison of metrics. Biol Psychol, 74(2), 243–262. doi:10.1016/j.biopsycho.2006.08.005 [PubMed: 17070982]

Allendorfer JB, Heyse H, Mendoza L, Nelson EB, Eliassen JC, Storrs JM, & Szaflarski JP (2014). Physiologic and cortical response to acute psychosocial stress in left temporal lobe epilepsy - A pilot cross-sectional fMRI study. Epilepsy Behav, 36C, 115–123. doi:10.1016/j.yebeh.2014.05.003

Arnsten AF (2015). Stress weakens prefrontal networks: molecular insults to higher cognition. Nat Neurosci, 18(10), 1376–1385. doi:10.1038/nn.4087 [PubMed: 26404712]

Arnsten AF, Raskind MA, Taylor FB, & Connor DF (2015). The Effects of Stress Exposure on Prefrontal Cortex: Translating Basic Research into Successful Treatments for Post-Traumatic Stress Disorder. Neurobiol Stress, 1, 89–99. doi:10.1016/j.ynstr.2014.10.002 [PubMed: 25436222]

Bach DR, Flandin G, Friston KJ, & Dolan RJ (2009). Time-series analysis for rapid event-related skin conductance responses. J Neurosci Methods, 184(2), 224–234. doi:10.1016/j.jneumeth.2009.08.005 [PubMed: 19686778]

Benjamini Y, & Hochberg Y (1995). Controlling the false discovery rate: A practical and powerful approach to multiple testing. Journal of the Royal Statistical Society. Series B (Methodological), 57(1), 289–300.

Chrousos GP (1998). Stressors, stress, and neuroendocrine integration of the adaptive response. Ann N Y Acad Sci, 851, 311–335. [PubMed: 9668623]

Chrousos GP (2009). Stress and disorders of the stress system. Nature Reviews Endocrinology, 5(7), 374–381. doi:10.1038/nrendo.2009.106

Chrousos GP, & Gold PW (1992). The concepts of stress and stress system disorders. Overview of physical and behavioral homeostasis. JAMA, 267(9), 1244–1252. [PubMed: 1538563]

Cisler JM, James GA, Tripathi S, Mletzko T, Heim C, Hu XP, . . . Kilts CD (2013). Differential functional connectivity within an emotion regulation neural network among individuals resilient and susceptible to the depressogenic effects of early life stress. Psychol Med, 43(3), 507–518. doi: 10.1017/S0033291712001390 [PubMed: 22781311]

Cohen JR, & D'Esposito M (2016). The Segregation and Integration of Distinct Brain Networks and Their Relationship to Cognition. J Neurosci, 36(48), 12083–12094. doi:10.1523/JNEUROSCI. 2965-15.2016 [PubMed: 27903719]

Cox RW (1996). AFNI: software for analysis and visualization of functional magnetic resonance neuroimages. Computers and Biomedical Research, 29, 162–173. [PubMed: 8812068]

David O, Guillemain I, Saillet S, Reyt S, Deransart C, Segebarth C, & Depaulis A (2008). Identifying neural drivers with functional MRI: an electrophysiological validation. PLoS Biol, 6(12), 2683–2697. doi:10.1371/journal.pbio.0060315 [PubMed: 19108604]

Dedovic K, Duchesne A, Andrews J, Engert V, & Pruessner JC (2009). The brain and the stress axis: the neural correlates of cortisol regulation in response to stress. NeuroImage, 47(3), 864–871. doi: 10.1016/j.neuroimage.2009.05.074 [PubMed: 19500680]

Dedovic K, Duchesne A, Engert V, Lue SD, Andrews J, Efanov SI, . . . Pruessner JC (2014). Psychological, endocrine and neural responses to social evaluation in subclinical depression. Soc Cogn Affect Neurosci, 9(10), 1632–1644. doi:10.1093/scan/nst151 [PubMed: 24078020]

Dedovic K, Renwick R, Mahani JK, Engert V, Lupien SJ, & Pruessner JC (2005). The Montreal Imaging Stress Task: using functional imaging to investigate the effects of perceiving and processing psychosocial stress in the human brain. Journal of Psychiatry and Neuroscience, 30(5), 319–325. [PubMed: 16151536]

Dedovic K, Rexroth M, Wolff E, Duchesne A, Scherling C, Beaudry T, . . . Pruessner JC (2009). Neural correlates of processing stressful information: an event-related fMRI study. Brain Res, 1293, 49–60. doi:10.1016/j.brainres.2009.06.044 [PubMed: 19555674]

Deshpande G, & Hu X (2012). Investigating effective brain connectivity from FMRI data: past findings and current issues with reference to granger causality analysis. Brain Connect, 2(5), 235–245. doi: 10.1089/brain.2012.0091 [PubMed: 23016794]

Deshpande G, Sathian K, & Hu X (2010). Effect of hemodynamic variability on Granger causality analysis of fMRI. NeuroImage, 52(3), 884–896. doi:10.1016/j.neuroimage.2009.11.060 [PubMed: 20004248]

Franklin TB, Saab BJ, & Mansuy IM (2012). Neural mechanisms of stress resilience and vulnerability. Neuron, 75(5), 747–761. doi:10.1016/j.neuron.2012.08.016 [PubMed: 22958817]

Ginestet CE, & Simmons A (2011). Statistical parametric network analysis of functional connectivity dynamics during a working memory task. NeuroImage, 55(2), 688–704. doi:10.1016/j.neuroimage. 2010.11.030 [PubMed: 21095229]

Goodman AM, Wheelock MD, Harnett NG, Granger DA, Mrug S, & Knight DC (2016). The hippocampal response to psychosocial stress varies with salivary uric acid level. Neuroscience, 339, 396–401. [PubMed: 27725214]

Gossett EW, Wheelock MD, Goodman AM, Orem TR, Harnett NG, Wood KH, & Knight DC (2018). Anticipatory stress associated with fMRI testing: a comparison between stress tasks performed inside and outside the scanning environment. International Journal of Psychoneuroendocrinology, 125, 35–41.

Granger CWJ (1969). Investigating causal relationships by econometric models and corss-spectral methods. Econometrica, 37, 424–438.

Granger DA, Fortunato CK, Beltzer EK, Virag M, Bright MA, & Out D (2012). Focus on methodology: salivary bioscience and research on adolescence: an integrated perspective. J Adolesc, 35(4), 1081–1095. doi:10.1016/j.adolescence.2012.01.005 [PubMed: 22401843]

Grant MM, Wood K, Sreenivasan K, Wheelock M, White D, Thomas J, . . . Deshpande G (2015). Influence of early life stress on intra- and extra-amygdaloid causal connectivity. Neuropsychopharmacology, 40(7), 1782–1793. doi:10.1038/npp.2015.28 [PubMed: 25630572]

Hartley CA, & Phelps EA (2010). Changing fear: the neurocircuitry of emotion regulation. Neuropsychopharmacology, 35(1), 136–146. doi:10.1038/npp.2009.121 [PubMed: 19710632]

Havlicek M, Friston KJ, Jan J, Brazdil M, & Calhoun VD (2011). Dynamic modeling of neuronal responses in fMRI using cubature Kalman filtering. NeuroImage, 56(4), 2109–2128. doi:10.1016/j.neuroimage.2011.03.005 [PubMed: 21396454]

Havlicek M, Jan J, Brazdil M, & Calhoun VD (2010). Dynamic Granger causality based on Kalman filter for evaluation of functional network connectivity in fMRI data. NeuroImage, 53(1), 65–77. doi:10.1016/j.neuroimage.2010.05.063 [PubMed: 20561919]

Hermans EJ, van Marle HJ, Ossewaarde L, Henckens MJ, Qin S, van Kesteren MT, . . . Fernandez G (2011). Stress-related noradrenergic activity prompts large-scale neural network reconfiguration. Science, 334(6059), 1151–1153. doi:10.1126/science.1209603 [PubMed: 22116887]

Holsen LM, Lancaster K, Klibanski A, Whitfield-Gabrieli S, Cherkerzian S, Buka S, & Goldstein JM (2013). HPA-axis hormone modulation of stress response circuitry activity in women with remitted major depression. Neuroscience, 250, 733–742. doi:10.1016/j.neuroscience.2013.07.042 [PubMed: 23891965]

Hosseini SMH, Hoeft F, & Kesler SR (2012). GAT: A graph-theoretical analysis toolbox for analyzing between-group differences in large-scale structural and functional brain networks. PLoS One, 7(7), e40709. doi:10.1371/journal.pone.0040709.g001 [PubMed: 22808240]

Jankord R, & Herman JP (2008). Limbic regulation of hypothalamo-pituitary-adrenocortical function during acute and chronic stress. Ann N Y Acad Sci, 1148, 64–73. doi:10.1196/annals.1410.012 [PubMed: 19120092]

Joels M, Pu Z, Wiegert O, Oitzl MS, & Krugers HJ (2006). Learning under stress: how does it work? Trends Cogn Sci, 10(4), 152–158. doi:10.1016/j.tics.2006.02.002 [PubMed: 16513410]

Kirschbaum C, Pirke K, & Hellhammer DH (1993). The 'Trier Social Stress Test' - a tool for investigating psychobiological stress responses in a laboratory setting. Neuropsychobiology, 28, 76–81. [PubMed: 8255414]

Kirschbaum C, Wolf OT, May M, Wippich W, & Hellhammer DH (1996). Stress- and treatment-induced elevations of cortisol levels associated with impaired declrative memory in healthy adults. Life Sciences, 58(17), 1475–1483. [PubMed: 8622574]

Knight DC, & Wood KH (2011). Investigating the neural mechanisms of aware and unaware fear memory with fMRI. Journal of Visualized Experiments, 56(e3083). doi:doi:10.39791/2083.

Leach J (2004). Why people 'freeze' in an emergency: temporal and cogntive constraints on survival responses. Aviation, Space, and Environmental Medicine, 75(6), 539–542.

Lupien SJ, Maheu F, Tu M, Fiocco A, & Schramek TE (2007). The effects of stress and stress hormones on human cognition: Implications for the field of brain and cognition. Brain Cogn, 65(3), 209–237. doi:10.1016/j.bandc.2007.02.007 [PubMed: 17466428]

Maldjian JA, Laurienti PJ, Burdette JB, & Kraft RA (2003). An automated method for neuroanatomic and cytoarchitectonic atlas-based interrogation of fMRI data sets. NeuroImage, 19, 1233–1239. [PubMed: 12880848]

McEwen BS, & Gianaros PJ (2011). Stress- and allostasis-induced brain plasticity. Annu Rev Med, 62, 431–445. doi:10.1146/annurev-med-052209-100430 [PubMed: 20707675]

McMenamin BW, Langeslag SJ, Sirbu M, Padmala S, & Pessoa L (2014). Network organization unfolds over time during periods of anxious anticipation. J Neurosci, 34(34), 11261–11273. doi:10.1523/JNEUROSCI.1579-14.2014 [PubMed: 25143607]

Negrao AB, Deuster PA, Gold PW, Singh A, & Chrousos GP (2000). Individual reactivity and physiology of the stress response. Biomedicine & Pharmacotherapy, 54, 122–128. [PubMed: 10840588]

Nicolaides NC, Kyratzi E, Lamprokostopoulou A, Chrousos GP, & Charmandari E (2015). Stress, the stress system and the role of glucocorticoids. Neuroimmunomodulation, 22(1–2), 6–19. doi:10.1159/000362736 [PubMed: 25227402]

Oken BS, Chamine I, & Wakeland W (2015). A systems approach to stress, stressors and resilience in humans. Behav Brain Res, 282, 144–154. doi:10.1016/j.bbr.2014.12.047 [PubMed: 25549855]

Quaedflieg CW, Meyer T, & Smeets T (2013). The imaging Maastricht Acute Stress Test (iMAST): a neuroimaging compatible psychophysiological stressor. Psychophysiology, 50(8), 758–766. doi: 10.1111/psyp.12058 [PubMed: 23701399]

Rubinov M, & Sporns O (2010). Complex network measures of brain connectivity: uses and interpretations. NeuroImage, 52(3), 1059–1069. doi:10.1016/j.neuroimage.2009.10.003 [PubMed: 19819337]

Schatzberg AF, Keller J, Tennakoon L, Lembke A, Williams G, Kraemer FB, . . . Murphy GM (2014). HPA axis genetic variation, cortisol and psychosis in major depression. Mol Psychiatry, 19(2), 220–227. doi:10.1038/mp.2013.129 [PubMed: 24166410]

Schwabe L, & Wolf OT (2010). Learning under stress impairs memory formation. Neurobiol Learn Mem, 93(2), 183–188. doi:10.1016/j.nlm.2009.09.009 [PubMed: 19796703]

Sousa N, & Almeida OF (2012). Disconnection and reconnection: the morphological basis of (mal)adaptation to stress. Trends Neurosci, 35(12), 742–751. doi:10.1016/j.tins.2012.08.006 [PubMed: 23000140]

Spielberger CD (1983). State-trait anxiety inventory for adutls. Mind Garder, RedwoodCity, CA.

Sreenivasan KR, Havlicek M, & Deshpande G (2015). Non-parametric hemodynamic deconvolution of fMRI using homomorphic filtering. IEEE Transactions on Medical Imaging, 34(5), 1155–1163. [PubMed: 25531878]

van der Werff SJ, Pannekoek JN, Stein DJ, & van der Wee NJ (2013). Neuroimaging of resilience to stress: current state of affairs. Hum Psychopharmacol, 28(5), 529–532. doi:10.1002/hup.2336 [PubMed: 23861065]

van Marle HJ, Hermans EJ, Qin S, & Fernandez G (2010). Enhanced resting-state connectivity of amygdala in the immediate aftermath of acute psychological stress. NeuroImage, 53(1), 348–354. doi:10.1016/j.neuroimage.2010.05.070 [PubMed: 20621656]

Vedhara K, Hyde J, Gilchrist ID, Tytherleigh M, & Plummer S (2000). Acute stress, memory, attention and cortisol. PNEC, 25, 535–549.

Veer IM, Oei NY, Spinhoven P, van Buchem MA, Elzinga BM, & Rombouts SA (2011). Beyond acute social stress: increased functional connectivity between amygdala and cortical midline structures. NeuroImage, 57(4), 1534–1541. doi:10.1016/j.neuroimage.2011.05.074 [PubMed: 21664280]

Veer IM, Oei NY, Spinhoven P, van Buchem MA, Elzinga BM, & Rombouts SA (2012). Endogenous cortisol is associated with functional connectivity between the amygdala and medial prefrontal cortex. Psychoneuroendocrinology, 37(7), 1039–1047. doi:10.1016/j.psyneuen.2011.12.001 [PubMed: 22204928]

Wang J, Wang X, Xia M, Liao X, Evans A, & He Y (2015). GRETNA: a graph theoretical network analysis toolbox for imaging connectomics. Front Hum Neurosci, 9, 386. doi:10.3389/fnhum. 2015.00386 [PubMed: 26175682]

Wang Y, Katwal S, Rogers B, Gore J, & Deshpande G (2016). Experimental validation of dynamic Granger causality for inferring stimulus-evoked sub-100 ms timing differences from fMRI. IEEE Transactions on Neural Systems and Rehabilitation Engineering, In Press.

Webb JT, Ferguson MA, Nielsen JA, & Anderson JS (2013). BOLD Granger causality reflects vascular anatomy. PLoS One, 8(12), e84279. doi:10.1371/journal.pone.0084279 [PubMed: 24349569]

Wheelock MD, Harnett NG, Wood KH, Orem TR, Granger DA, Mrug S, & Knight DC (2016). Prefrontal cortex activity is associated with biobehavioral components of the stress response. Front Hum Neurosci, 10, 583. doi:10.3389/fnhum.2016.00583 [PubMed: 27909404]

Wheelock MD, Sreenivasan K, Wood KH, Ver Hoef LW, Deshpande G, & Knight DC (2014). Threat-related learning relies on distinct dorsal prefrontal cortex network connectivity. NeuroImage.

Xia M, Wang J, & He Y (2013). BrainNet Viewer: A network visualization tool for human brain connectomics. PLoS One, 8(7), e68910. doi:10.1371/ [PubMed: 23861951]

Zhang J, Wang J, Wu Q, Kuang W, Huang X, He Y, & Gong Q (2011). Disrupted brain connectivity networks in drug-naive, first-episode major depressive disorder. Biol Psychiatry, 70(4), 334–342. doi:10.1016/j.biopsych.2011.05.018 [PubMed: 21791259]

Zhang W, Li H, & Pan X (2015). Positive and negative affective processing exhibit dissociable functional hubs during the viewing of affective pictures. Hum Brain Mapp, 36(2), 415–426. doi: 10.1002/hbm.22636 [PubMed: 25220389]

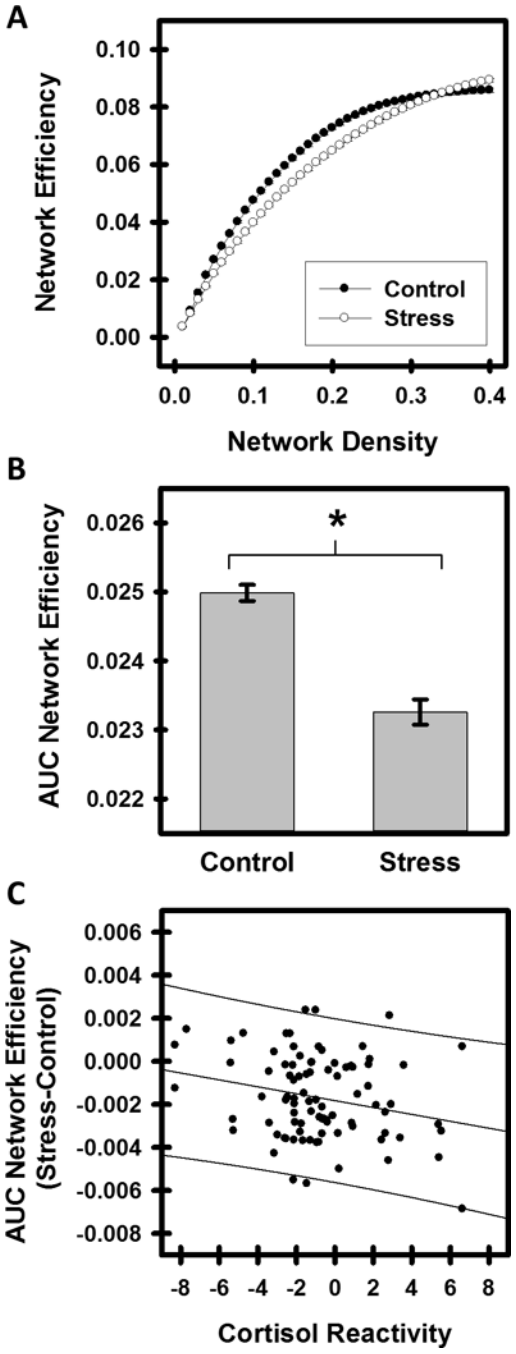

Figure 1.

Network Efficiency during Control and Stress conditions. Network efficiency (Mean±SEM) was significantly lower during the Stress than Control condition at a range of network densities (A). The area under the curve (AUC) estimate of network efficiency demonstrated lower network efficiency during the Stress than Control condition ($t(90)=-8.16$, $p<0.001$) (B). Differential network efficiency (Stress-Control) negatively correlated with cortisol reactivity ($r=-0.282$, $p=0.004$) (C). A greater stress response was observed in participants with lower network efficiency during Stress compared to Control conditions.

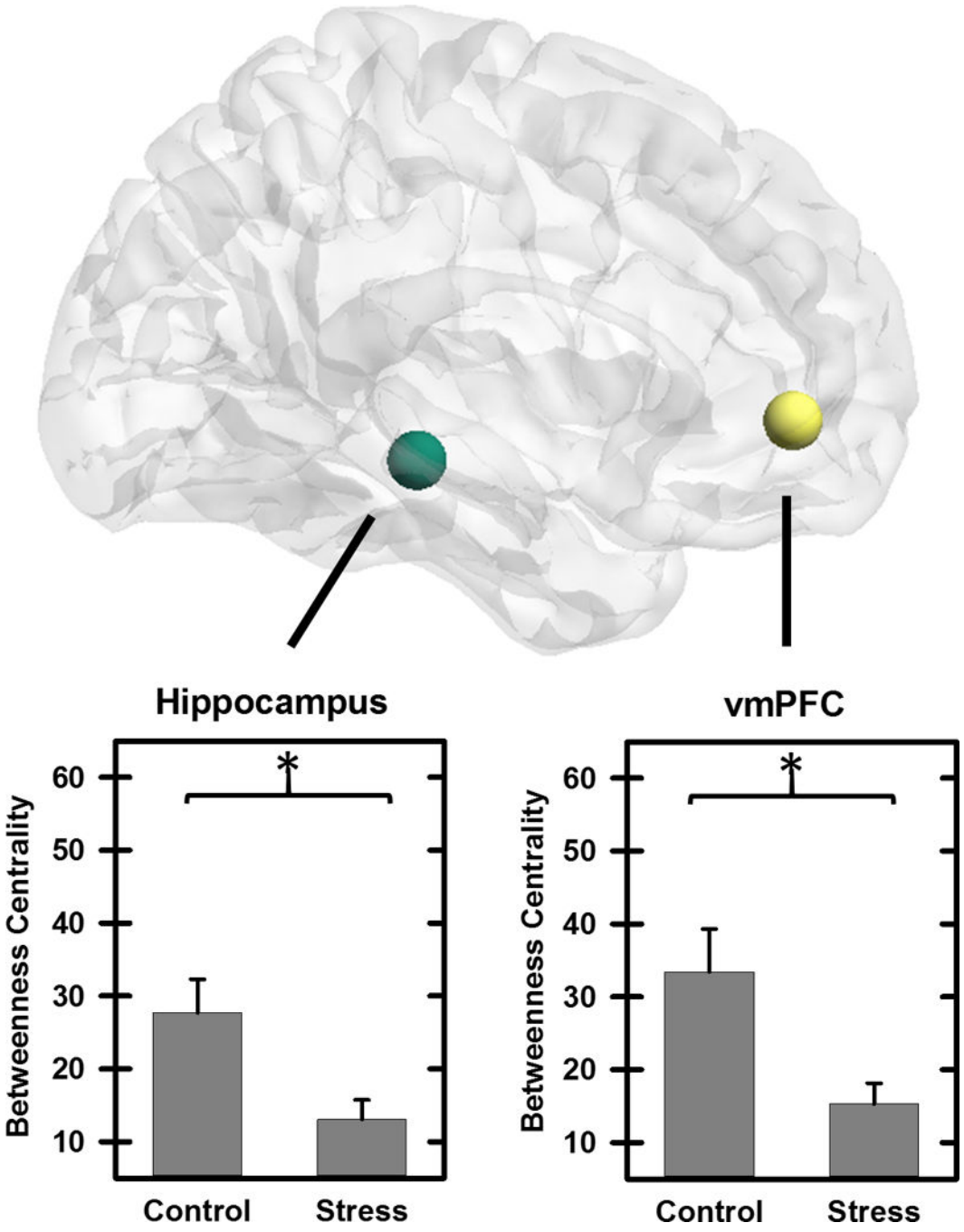

Figure 2.

Betweenness centrality during Control and Stress MIST. Betweenness centrality was assessed for an *a priori* set of 12 regions including ventromedial prefrontal cortex, cingulum, amygdala, and hippocampus. Decreased betweenness centrality was observed during Stress compared to Control conditions within the hippocampus and ventromedial prefrontal cortex (vmPFC) ($p<0.05$ FDR corrected).

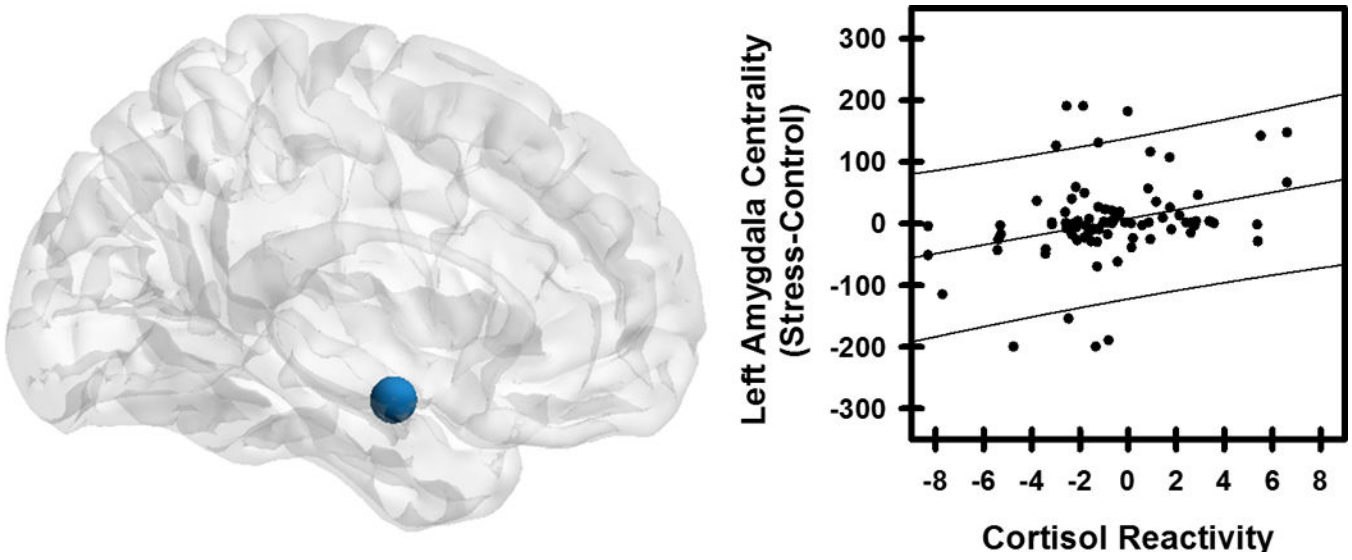

Figure 3.

Node centrality and psychobiological data. A positive relationship was observed between differential left amygdala node betweenness centrality and cortisol reactivity (r=0.302, *p*=0.002). Individuals in which the amygdala was more central to network information transfer had a greater stress response.

Table 1.

Paired samples t-tests comparing Control to Stress MIST

Measure	Control (M±SEM)	Stress (M±SEM)	n	*t*	*p*
Response time	2.87±0.04	2.16±0.04	108	−26.62	0.001
% correct responses	86%±1%	54%±0.1%	108	−36.89	0.001
Stress Rating	13.91±0.54	27.38±0.67	96	16.28	0.001
SCR	0.39±0.04	0.95±0.07	89	8.30	0.001
HR	67.26±1.12	73.94±1.61	69	6.52	0.001

Response time (in seconds) indicates time following math problem presentation to response selection with a button press. HR, Heart Rate; SCR, Skin Conductance Response. Stress ratings were not collected on 12 participants. Thirteen participants had errors in HR data acquisition, and 26 participants had HR with low SNR. Nineteen subjects did not have any SCRs above 0.05 μSiemens. SEM reflects within subject standard error of the mean.

Table 2.

Global network efficiency and psychobiological responses

		Efficiency$_g$ During Stress		**Efficiency$_g$ Stress-Control**	
	n	**r**	**p**	**r**	**p**
Psychological					
Self-Reported Stress	80	0.141	0.106	0.140	0.108
Trait Anxiety	91	−0.147	0.082	−0.181	0.043
Biological					
Heart Rate Reactivity	58	0.120	0.185	0.147	0.136
SCR Reactivity	77	−0.168	0.072	0.02	0.431
Cortisol Reactivity	89	−0.282	**0.004** *	−0.238	0.012

Efficiency$_g$, Global Network Efficiency; SCR, skin conductance response.

* represents significance at FWE p<0.05, one-tailed.

Table 3.

Betweenness centrality analyses of *a priori* nodes

Region	Control M±SEM	Stress M±SEM	*t*	p_{FDR}
Left amygdala	26.11±5.06	28.22±5.81	−0.279	0.781
Right amygdala	41.61±5.94	30.00±5.70	1.298	0.339
Left hippocampus1	27.68±4.61	13.07±2.64	2.906	**0.030** *
Left hippocampus2	27.15±5.04	25.07±5.08	0.283	0.781
Left rACC	31.98±4.91	17.54±3.29	2.520	0.052
Left vmPFC	33.40±5.88	15.29±2.86	2.887	**0.030** *
Left medial OFC	36.33±6.42	25.48±5.11	1.312	0.339
Right medial OFC1	25.39±7.30	18.79±5.29	0.720	0.631
Right medial OFC2	20.32±4.18	18.26±3.55	0.476	0.763
Left dACC1	22.74±4.41	16.24±3.58	1.120	0.399
Left dACC2	33.02±5.90	19.55±3.74	1.875	0.154
Right dACC	36.98±5.11	21.63±4.35	2.324	0.066

rACC, rostral anterior cingulate cortex; vmPFC, ventromedial prefrontal cortex; OFC, orbitofrontal cortex; dACC, dorsal anterior cingulate. *p*-values are FDR adjusted.

* indicates significant p-values after FDR ($p<0.05$) correction.

Table 4.

Amygdala betweenness centrality correlated with psychobiological responses

		Betweenness During Stress		Betweenness Stress-Control	
	n	**r**	**p**	**r**	**p**
Psychological					
Self-Reported Stress	80	0.131	0.123	−0.083	0.233
Trait Anxiety	91	0.047	0.329	0.070	0.255
Biological					
Heart Rate Reactivity	58	−0.298	0.012	−0.186	0.082
SCR Reactivity	77	−0.028	0.404	−0.144	0.106
Cortisol Reactivity	89	0.155	0.074	0.302	**0.002** *

Self-reported stress represents the differential stress rating (Stress-Control conditions).

* indicates significance at FWE corrected $p<0.05$, one-tailed.